Thomas Jefferson National Accelerator Facility

JLAB 2000-draft-01
June 10, 2000

Letter of Intent

Presented by J.-M. Laget and E.Chudakov

Abstract

This letter of intent discusses the physics motivations to measure the charm photoproduction close to the threshold and possible experiments on this subject with the 12 GeV beam at JLab.

1 Experimental program on charm production

The physics program discussed includes the topics as follows:

- Measurements of the energy dependence of charm photoproduction differential cross-section, in an energy range of 8.5-11 GeV, on protons.
- Measurements of Ψ-Nucleon cross-section. This measurement can be done at the highest energy available, using several target materials.
- A search for rare effects, like the “hidden color” is of considerable interest. “Hidden color” can manifest itself in the $J/\psi(1S)$ production on deuterium.

The measurements of the first item might be carried out in several ways. As far as the theoretical predictions are concerned, the full charm production is easier to interpret than the charmonia production, since the final state interaction can be neglected in the former case but may play an important role for the latter. On the experimental side, it is easier to detect charmonia, and $J/\psi(1S)$ in particular, than the full charm production, which would require a detection of several types of charmed particles like $\overline{D}^0$ and $D^{\pm}$ on a typically higher background level.

#	reaction	E_γ GeV threshold	useful decay mode	BR	E_γ, GeV	σ nb
1	$\gamma p \rightarrow \eta_c(1S)p$	7.7 GeV	$\eta_c(1S) \rightarrow \gamma\gamma$	0.03%	-	-
			$\eta_c(1S) \rightarrow p\overline{p}$	0.12%	-	-
2	$\gamma p \rightarrow J/\psi(1S)p$	8.2 GeV	$J/\psi(1S) \rightarrow e^-e^+$	6.0%	11.	0.5±0.2
			$J/\psi(1S) \rightarrow \mu^-\mu^+$	6.0%		
3	$\gamma p \rightarrow \Lambda_c^+\overline{D}^0$	8.7 GeV	$\overline{D}^0 \rightarrow K^+\pi^-$	4.0%	20.	$\sim$ 63.±30.
4	$\gamma p \rightarrow \Lambda_c^+ D^*(2010)^0$	9.4 GeV	$D^*(2010)^0 \rightarrow \overline{D}^0 X$	100.0%	20.	$\sim$ 63.±30.
5	$\gamma p \rightarrow \Sigma_c^+ D^-$	9.5 GeV			20.	
6	$\gamma p \rightarrow \chi_{c0}(1P)p$	9.6 GeV	$\chi_{c1}(1P) \rightarrow K^+K^-$	0.71%		
7	$\gamma p \rightarrow \chi_{c1}(1P)p$	10.1 GeV	$\chi_{c1}(1P) \rightarrow J/\psi(1S)\gamma$	27.0%	90.	$<$ 7% J/Ψ
8	$\gamma p \rightarrow \chi_{c2}(1P)p$	10.3 GeV	$\chi_{c1}(1P) \rightarrow J/\psi(1S)\gamma$	13.0%	90.	$<$ 27% J/Ψ
9	$\gamma p \rightarrow \psi(3770)p$	11.0 GeV	$\psi(3770) \rightarrow e^-e^+$	0.8%	21.	1.1±0.4
			$\psi(3770) \rightarrow \mu^-\mu^+$	0.8%		
10	$\gamma p \rightarrow D\overline{D}p$	11.1 GeV			20.	$\sim$ 63.±30.

Table 1: The thresholds of several channels of charm photoproduction reactions reside in the energy range from 8 to 12 GeV. The thresholds of similar reactions with an additional pion are about 0.6 GeV higher. The decays modes, convenient for detection and their branching ratios are shown. The last columns indicates whether this reaction has been detected in photoproduction at low energies and the cross-section measured. The open charm cross-section measurement was inclusive. The cross-section of a particular channel is a part of the full one of 63±30 nb.

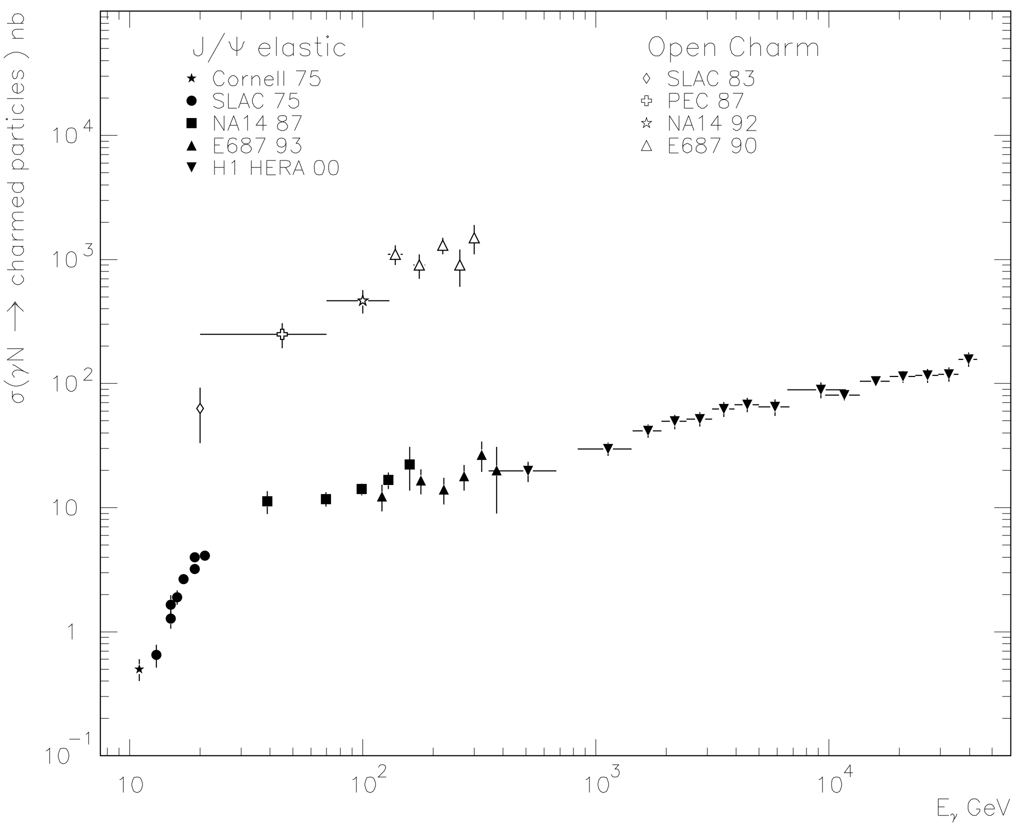

Figure 1: A sample of the existing data on J/ψ(1S) and open charm photoproduction cross-sections in a wide range of energies [4, 5, 6, 7, 9, 10, 11, 12, 13, 14, 15, 16, 17, 18, 19, 20] The ratio between open charm and J/ψ(1S) varies from 10 at 20 GeV to 100 at 300 GeV.

A number of various channels of charm photoproduction on the nucleon open between 8 and 12 GeV (see Table 1). The cross-section of open charm photoproduction at 20 GeV [11, 12] is about 10 times higher than the J/ψ(1S) production [4] (see Figure 1). Therefore the J/ψ(1S) production may be affected somewhere above the open charm threshold of 8.7 GeV. There are no data on the open charm photoproduction below 20 GeV. It would be interesting to measure the open charm cross-section in the same energy range as J/ψ(1S). In a range from 8.7 to about 9.4 GeV the open charm necessarily includes a $\overline{\mathrm{D}}^0$, while above that energy D^- can be also produced. D^+or D^0can not be produced below the $\mathrm{D}\overline{\mathrm{D}}$ threshold of 11.1 GeV.

The lowest threshold reaction involving charm is η_c(1S) production. Unfortunately, the branching ratios of this particle's 2-body decay modes are very low, which may explain why it has not been observed in photoproduction up to now. An upper limit of about 30 nb was measured at 11 GeV [21], with the $\gamma\gamma$ decay mode.

Another interesting process would be the $\chi_{c1}(1P)$ production. So far, an upper limit for the ratio of $\chi_{c1}(1P)$ to $J/\psi(1S)$ cross-sections of 7% was measured at about 90 GeV [15]. On the other hand, in hadroproduction about 30% of all $J/\psi(1S)$ come from χ_c particles [22].

The measurement of Ψ-Nucleon cross-section involves measurements of $J/\psi(1S)$ production cross-section on several nuclear targets, from which one can extract the Ψ-Nucleon cross-section using the Glauber methods. The "hidden color" can be looked for in $J/\psi(1S)$ production on deuterium and requires a high sensitivity. Therefore, all the tasks discussed are technically similar to each other, though different targets should be used.

The program require very sensitive experiments, also providing reasonably low systematic errors. The existing $J/\psi(1S)$ data [4, 5] at low energy has a systematic error due to an inelastic component of the production. This component was estimated as about 30%. The new experiment should be able to identify the recoil particle in order to identify the elastic production.

In order to decide on the best strategy for these measurements, the experimental methods to detect the charmed particles should be considered.

2 Experimental ways to detect charmed particles

Detecting charmed particles is difficult, in particular at low energies, because of a low production cross-section (below 1 nb) and low branching ratios of the decay modes convenient for detection (a few percent). The cross-section at the lowest energy point can be as low as 0.005 nb. One can compare the photoproduction of $J/\psi(1S)$ at 11 GeV with the photoproduction of $\phi(1020)$ in an energy range of 2-4 GeV. The yield of $J/\psi(1S)\to e^+e^-$ is about 10^{-4} of the $\phi(1020) \to K^+K^-$ yield.

Nevertheless, several experiments have proven that charm detection at low energies is possible. The key signatures for charm are:

1. small or zero (for particles decying weakly) particle widths;
2. high free energy of 2-body decays;
3. short, but detectable decay paths of weakly decaying particles;
4. semileptonic decays have relatively high probabilities of $\sim 10\%$;
5. decays of the associated charmed particle may provide an additional signature.

For charmonia, only the items 1 and 2 are valid. The reliable way to identify a photoproduced charmonium is to observe an appropriate peak in the mass distribution of its decay products. The lowest background is usually observed for 2-body decays with the highest free energy. For the decays to a lepton pair like e^+e^- or $\mu^+\mu^-$ the main background comes from the Bethe-Heitler process. Hadronic decays of charmonia have many particles in the final state and a high combinatorial background. The experiment should provide as high mass resolution as possible and a reasonably good identification of leptons. This technique worked out down to low energies, namely at 13-20 GeV at SLAC [4] and at 11. GeV at Cornell [5]. The former experiment used the SLAC high resolution spectrometers and observed about 1200 $J/\psi(1S)$ particles on a very low background, while the latter used a calorimeter to detect the e^+e^- decays, providing a mass resolution about 10 times worse than the SLAC experiment, and observed about 500 $J/\psi(1S)$ on a 20% background. There were experiments at SLAC detecting only one lepton from $J/\psi(1S)$ decays [7]. This method based on subtraction of a calculated background did not work well at energies below 11-13 GeV because of a high background level [8].

Identification of open charm is also based on a good mass resolution, and the lowest background has been observed for 2-body decays of D^0. Additionally, the items 3-5 are valid. At high energies, where the charm cross-section is higher than 50 nb, measuring the decay path of charmed particles (0.5-10 mm) became a very successful technique to identify charm. The lowest energy at which the open charm has been observed in photoproduction is 20 GeV, using a high resolution bubble chamber at SLAC [11, 12], measuring the decay paths. Unfortunately, all the vertex detector techniques are poorly compatible with very high luminosity experiments, needed to measure a cross-section of about 0.01 nb. In a number of experiments, the detection of the semileptonic decays of the associated particle helped to reduce the background by a factor of several. However, the charm signal is reduced by a factor of at least 10, which makes such a technique not attractive at low energies. One might consider an experiment detecting only one lepton from the semileptonic decays. Such an experiment, providing a high rate, would be based on subtraction of the calculated background imposing a large systematic error.

At the energies of 20-70 GeV [9] D^0production has been measured, on a thick 67 cm hydrogen target and without a special tagging, using a spectrometer with a mass resolution for $D^0$of about $\sigma M/M \approx 0.5\%$. The signal to background ratio observed was about 1/5. In order to see charm at low energies one should provide a considerable improvement of the mass resolution. Detecting the $D^\pm$ or charmed baryons can be more difficult, since the detectable decays include at least 3 charged particles in the final state and one may expect a higher combinatorial background. Such higher backgrounds were indeed observed in a number of experiments.

With a tagged photon beam it is possible to identify a 2-body reaction detecting only one final state particle. This would identify the "elastic production" of quarkonia on protons. With the open charm, one can identify the associated charmed particle by measuring the missing mass and therefore reduce considerably the background. With an untagged beam one can identify a 2-body reaction by detecting the recoil proton along with the quarkonium, and selecting the "elastic production" kinematically. Identifying a certain open charm reaction in an untagged beam is more problematic since the associated particle most likely stays unidentified.

3 Experiments on charm at JLab

In this section different options for the charm studies at JLab are discussed. It is evaluated whether the standard JLab equipment would be adequate to the task, or a new detector should be built in order to fulfill the program.

3.1 Simulation

In order to evaluate the acceptance, resolution and the statistical accuracy of possible experiments a simple simulation of charm production and detector performance was done.

The kinematics of photoproduction of $J/\psi(1S)$ was described by a differential cross-section as:

$$\frac{d\sigma}{dt} = A \cdot (1-x)^n \cdot e^{\beta t} \tag{1}$$

with β=1.0 $(\mathrm{GeV/c})^{-2}$ and n=2. The value of x is define in **??**. The cross-section for $J/\psi(1S)$ was normalized to the measurements at 11 [5] and 13 GeV [4], so at 11 GeV the full cross-section was 0.32 nb. For the open charm the same differential cross-section was taken, scaled by a factor of 10.

The angular distribution of $J/\psi(1S)$ leptonic decays were simulated assuming helicity conservation: $(1+\cos^2\theta_{CM})$.

For simulation of the standard JLab spectrometers no particle tracking and interaction with media was simulated. The decay probability of charged kaons was taken into account. The acceptance was supposed to be flat within certain windows.

Simulation of a new setup was done using GEANT.

The acceptance and the mass resolution were calculated. In order to estimate the particle yield additional factors were considered:

- 0.5 - efficiency of the trigger, event reconstruction etc;
- 0.7 - beam delivery efficiency.

3.2 Measuring the photon energy

In order to measure a steep energy dependence of the cross-section the energy bins used should be small enough that the cross-section does not change for more than a factor 3-5 within the bin. Assuming the cross-section described by Formula (1) one would define a maximum bin size of about 0.4 GeV. This requires that the photon energy should be measured with a precision better than $\sim$0.1 GeV.

For a tagged beam, like one designed for Hall D, the photon energy resolution is about 0.1%, which is more than enough. For an untagged beam, one can derive the incident photon energy from the kinematics of the observed particle ($J/\psi(1S)$ or D), assuming a certain 2-body reaction. Using the known mass of $J/\psi(1S)$ and its decay kinematics one can considerably improve the resolution. If the typical double arm JLab spectrometers are used to detect the products of a 2-body decay a resolution of about 0.2% can be achieved.

A certain 2-body reaction is defined if either the other particle (say, proton for $J/\psi(1S)$ "elastic production") has been detected or only one reaction is allowed for the given end point energy of the photon beam.

3.3 Background estimates

Because of the low cross-section of charm production the level of background is a very important item limiting the ability to extract charm signals and the statistical accuracy one can achieve.

The Cornell experiment [5], providing a mass resolution for $J/\psi(1S)\rightarrow e^+e^-$ of 5%, observed a signal to background ratio of about 5/1 with 11. GeV photons on beryllium. Most of the background was described by the Bethe-Heitler process. We assume that the experiments we consider at JLab would have the similar power to identify electrons like the Cornell experiment. So, we used the same signal to background ratio, scaled for the mass resolution of the experiment considered, and assumed that this background at a mass of 3.1 GeV/c^2 scales with the beam energy in the same way as the $J/\psi(1S)$ cross-section. We also assumed that at the Cornell conditions there was a 5% background independent on the beam energy. The same background was considered for $J/\psi(1S)\rightarrow\mu^+\mu^-$.

The 2-body decay of $\overline{D}^0$ is a more difficult task if no background suppression technique, like measuring the decay paths, is used. An experiment [9] in a photon beam of 20-70 GeV on a 67 cm long liquid hydrogen target, with a mass resolution of 0.5%, observed a signal to background ratio of about 1/5. At the moment we do not know how this background would scale with the beam energy. The background would depend on the power to identify charged kaons.

For a tagged beam there is an independent way to reduce the background by selecting a certain 2-body reaction with the missing mass calculation. This technique could be useful at low energies. Above the beam energy of 9.4 GeV one extra pion can be produced and at higher energies the 2-body reactions define a small part of the full charm cross-section.

For the moment we assumed that at 11 GeV the signal/background for D-meson search is 1/5 and that the one half of this background scales with the energy like the charm cross-section, while the other half does not depend on the energy.

3.4 Charm studies using the JLab standard spectrometers

The parameters of the existing or planned JLab spectrometers are shown in Table 2.

It was assumed that Halls A and C would use a 11 GeV 40μA beam on a 6% radiator, which provides a photon flux of about $1.2\cdot10^{12}\gamma$/s/GeV. For Hall D [23] it was assumed that the coherent bremsstrahlung flux has a trapezoidal shape and ranges from 8.5 to 9.1 GeV, while the incoherent component is flat in a range of 8.2-11 GeV, and that both components have the same total fluxes of $2\cdot10^7\gamma$/s in the ranges given.

hall	beam μA	setup	$\Delta\Omega$ ster	P$_{max}$ GeV	$\frac{\Delta P}{P}$ %	$\frac{\sigma P}{P}$ %	$\sigma\theta_{inplane}$ mrad	$\sigma\theta_{outplane}$ mrad
Hall A	40	HRS	0.006	4.0	9	0.01	0.6	2.0
		HRS	0.006	3.2	9	0.01	0.6	2.0
		MAD	0.030	6.0	15	0.3	1.0	2.0
Hall C	40	HMS	0.006	7.5	18	0.1	0.8	0.8
		SOS	0.009	1.8	40	0.1	1.0	1.0
		SHMS	0.003	12.	18	0.1	1.0	1.0
Hall D	γ		$\sim 4\pi$	-	-	<1.		

Table 2: The parameters of the existing or planned spectrometers. MAD (Medium Acceptance Device) is a spectrometer being designed for Hall A. This spectrometer would have a variable position along the beam, allowing to reduce the minimal angle while loosing the acceptance. The second column indicate the maximum beam current which the accelerator can provide at 12 GeV and allowed by the hall environment. The photon flux of Hall D is discussed in the text. Since the Hall B CLAS abilities for charm detection are unlikely better than those of Hall D, they have not been evaluated here.

The photon energy range was split into 0.4 GeV bins. Halls A and C are using an untagged beam and have no means to detect the recoil particle (proton for J/ψ(1S) production). Therefore one can not be sure of the reaction observed and of the photon energy. One has to make measurements at several endpoints matching the energy bins, and obtain the result for a given bin by subtraction. The exposition time given for every point was optimized assuming the cross-section (1) by minimizing the maximum error of all the bins except the first one (the lowest energy bin).

The results of calculations are summarized in Table 3.

The best results can be obtained by Hall D and the MAD+HRS spectrometers of Hall A. The expected measurements with their errors are presented on Figure 2. Although Hall D has a lower sensitivity than MAD+HRS, it has a considerable advantage of the beam tagging and of a large acceptance which allow to select certain 2-body reactions, including the "elastic" production of J/ψ(1S).

3.4.1 Summary on the standard spectrometers

- J/ψ(1S) studies:
  - ∘ Halls A/C (mainly HRS+MAD):
    - \+ enough statistics for $\sigma >\sim 0.01$nb;
    - – the recoil particle is not detected;
    - – the decay angular distribution not measured - no polarization study is possible.
  - ∘ Hall D has some advantages:
    - \+ the recoil and other particles are detected;

meaning	Hall D	HRS HRS	HRS MAD	HMS SOS	HMS SHMS
tagged γ	yes				
target LH	30 cm	15 cm	15 cm	4 cm	15 cm
J/ψ(1S)$\to$ e$^+$e$^-$,$\mu^+\mu^-$					
$E_\gamma range$ GeV	8.3-11.	8.3-11.	8.3-11.	8.3-9.5	8.3-11.
decay angle CM	-	-	100^o	51^o	90^o
Acceptance %	~ 40	-	0.027	0.026	0.009
$\sigma M/M$	$\sim 1\%$	-	0.24%	0.2%	0.2%
events/90days	390	-	4100	230	1400
days required*	250	-	90	-	260
$\overline{\mathrm{D}}^0 \to$K$^+\pi^-$					
$E_\gamma range$ GeV	8.7-9.3	8.7-11.	8.7-11.	8.7-10.	8.7-11.
decay angle CM	-	90^o	100^o	66^o	80^o
Acceptance %	~ 40	0.003	0.022	0.026	0.008
$\sigma M/M$	$\sim 1\%$	0.17%	0.2%	0.2%	0.2%
events/90days	870	900	5600	370	2000

Table 3: The prospects of the charm studies with the standard JLab equipment. The decay angle accepted may be constrained for 2-arm spectrometers due to their limitations on the minimum angle and maximum momentum. Measurements by 2-arm spectrometers have to be done at several endpoints with a 0.4 GeV step. The number of days required was estimated for a condition that the relative statistical error averaged for all the bins except the first one does not exceed 10%. This estimate was not done for D production since for the moment we have no reliable estimate of the background level

+ the angular distribution is measured;

+ the photon energy is known and no end point tunes are needed;

– about 2 years running is needed;

+ running parallel with the other programs.

- Open charm studies:
  - ◦ results are dependent on the level of background (no experimental data exists on this matter);
  - ◦ halls A (HRS+MAD) has a statistical advantage over Hall D and needs 3-5 months to make a useful measurement, while Hall D may be able to reduce the background.

The existing equipment may be enough for a cross-section measurement on one target (Hydrogen) for both J/ψ(1S) and open charm, in case the cross-section does not fall steeper than $(1-x)^2$. It would not be possible to measure the rare effects like hidden color. MAD+HRS can study the A-dependence of the J/ψ(1S) cross-section, in order to extract the Ψ-nucleon cross-section, with additional time allocated various nuclear effects etc. Also it is not enough for looking for $\chi_{c1}(1P)$ or $\eta_c(1S)$

3.5 A dedicated apparatus for $J/\psi(1S)$ studies

The existing equipment if JLab may be able to make a pilot experiment and obtain results on the $J/\psi(1S)$ production with a statistical accuracy of about 10%. In order to fulfill the most challenging part of the program a considerable improvement is needed. It would be difficult to improve considerably the prospects for open charm studies at JLab. However it is possible to make a major improvement of $J/\psi(1S)$ studies, building a dedicated detector, which:

- capable to work at a luminosity of $\mathcal{L} \sim 10^{36}$;
- has a high acceptance of >0.2;
- detects Ψ and the recoil proton;
- detects a wide range of the decay angles: $-0.5 < \cos\theta_{CM} < 0.5$.

3.5.1 Outline

The momentum and the angular ranges of the recoil proton are similar to those of the $J/\psi(1S)$ decay products, but the proton direction is practically uncorrelated with them. In order to provide a reasonable acceptance, a large acceptance recoil detector should be used. Such a detector would not work with the high resolution spectrometers (MAD+HRS), because of the high luminosity. On the other hand, the luminosity at the large acceptance detector of Hall D is limited both by the beam tagging and by the detector geometry and types.

Here we consider a detector operating in an untagged beam of about 1000 times higher rate than the beam of Hall D, with an acceptance smaller than the acceptance of the Hall D detector (limited in the polar angle), but still not lower than 10%.
Let us consider a detector consisting of:

- A calorimeter for detecting e^+e^-: the energy and the coordinates are measured.
- A scintillator or lucite hodoscope in front of the calorimeter.
- Protons are detected/identifies using the calorimeter and a scintillator detector behind.
- Tracking would be of a big help in order to reduce the accidental rate (in a long target) reconstructing the proton tracks;
- A magnetic field should be used, mainly in order to remove the low energy electrons.

The limitations on the luminosity that such a detector can take in electron on photon beams are driven by:

- The detectors:
  - the maximum allowed energy flow/s/module in the calorimeter;
  - the maximum allowed charged particle flux/s/cm^2 in the tracking detectors;

– the maximum allowed occupancy in the tracking detectors;
– the maximum allowed charged particle flux/s/module in the trigger hodoscope;

- The trigger rate should be $< 2 \cdot 10^4$/s.

- The accidental coincidence:

– CEBAF defines a minimum resolution time of 2ns;
– Track reconstruction with an extended target would provide a factor of >10 improvement.

A successful experiment at Cornell [5] used 2 arrays of a lead-glass calorimeter at a distance of 150cm from the target. The low energy background was removed with a help of a dipole magnet providing a field integral of 0.85 kGs·m. Using a dipole field makes a dead zone along a central band, normal to the field, thus reducing the acceptance. We preferred to consider a solenoidal field and a detector homogeneous in the azimuthal angle. The strength of the field should be selected on the base of the low energy background suppression.

A sketch of the detector is presented on Figure 3. The experiment uses a mixed beam. A radiator of 6% radiation length is positioned at about 130cm from the target center. A shielding 80 cm long downstream of the radiator helps to absorb the particles coming from the radiator at high angles. Various targets should be used - liquid hydrogen (about 10 cm long), liquid deuterium and solid targets. The target is positioned in a solenoidal magnetic field. The acceptance of the detector in the polar angle θ ranges from 10° to 30°, which covers the decay angles in the $J/\psi(1S)$ CM frame of $0.5 < \cos\theta_{CM} < 0.5$. The magnetic field fills most of the volume up to the calorimeter, 150 cm downstream of the target. The ring-shaped tracking detectors are positioned between the target and the calorimeter. For proton identification, a thick scintillator hodoscope (not shown on Figure 3) can be installed downstream of the calorimeter. The choice of the detectors is discussed in the next sections.

3.5.2 The choice of the magnetic field

The field would play two roles. The first and the most important is to contain the low energy charged background to the central area close to the beam, at angles below 10°. The second role is to help measuring the track momenta, in particular for the recoil protons. The field was optimized using GEANT [27] simulation, which simulated the electron beam interaction in the radiator and in the target and tracked the particles through the setup. The energy fluxes through the detector planes were estimated. In order to check the accuracy of GEANT simulation of the energy flux, we compared the results of simulations with a measurement done in Hall A. The measurement was done with a 1.833 GeV beam on a 15 cm liquid hydrogen target, at 11° using a lead-glass calorimeter module. The measured energy flux was about 25% lower than the predicted by GEANT. This agreement is sufficiently good.

The results of the calculations of the energy flux at the face of the calorimeter are shown on Figure 4. The optimal field is about 2 T. Higher fields practically would not help to reduce the energy flux, but would help the momentum measurements.

3.5.3 Calorimeter

Lead-glass calorimeters have been widely used for high flux environment. They have a typical energy resolution of about $\sigma E/E \approx 0.06\ \mathrm{GeV}^{0.5}/\sqrt{E}+0.01$ and a position resolution of several mm, depending on the lateral size of the module. Lead-glass calorimeters detect Cherenkov light and are not sensitive to low energy background which is below the Cherenkov threshold. The minimal lateral size of a module, defined by the Molière radius, is typically about 4 cm.

The maximum energy flow which a calorimeter can stand was defined as the flow causing a shift of the pedestal corresponding to about 1% of the minimal energy to be measured. Assuming the minimal energy of 2 GeV and a gate of 100 ns on the ADC, one obtains the maximal flux allowed of 2×10^5GeV/s/module. At Hall A, various tests of lead-glass calorimeter prototypes have been made and it was found that indeed at the conditions given the calorimeter was operating normally.

Since we have to minimize the energy flow per module, we are also considering a heavier material calorimeter for the central part of the array. At the moment the most attractive candidate is $PbWO_4$ crystal with Molière radius of 2.2 cm - about 1/2 of the typical lead-glass. This allows to build modules of about 2×2 cm^2. The energy resolution is 2-3 times better than the lead-glass resolution. Since the $PbWO_4$ crystal scintillates it may be more sensitive to the low energy flux. The behavior of the crystal in the environment of a high luminosity experiment should be studied experimentally.

Let us assume that the size of the modules at the low angles is 2×2cm^2. From the Figure 4 we see that at the 2 T magnetic field at a radius of 27 cm, or $\theta = 10^\circ$, the flux through such a module should be about $3\cdot10^4$GeV/s at $1\mu A$, which is about 15% of the limit. With no field the flux would be about $1.5\cdot10^6$GeV/s, which is about 7 times higher than the limit. At the radius of about 45 cm the flux drops by a factor of 4-5. Therefore the small $PbWO_4$ modules should cover a ring between the radii 27 and 45 cm. The outer area can be covered with lead-glass modules of 4×4cm^2.

The full number of modules needed for the detector depicted on Figure 3 is 1136 of lead-glass and 1028 of $PbWO_4$.

The calorimeter described should be able operate at the beam currents up to $\sim 6\mu$A.

3.5.4 Tracking detectors

So far, the best detector for the experiment discussed is GEM (Gas Electron Multiplier) detector [24, 25, 26]. This detector was invented at CERN in about 1996, as an improvement of the MSGC (Micro Strip Gas Chamber) and its technology is quickly maturing. The parameters are:

- It stands high particle densities $\sim 10^7/\text{cm}^2/\text{s}$.
- A small pitch of 200-400μm helps to keep the occupancy acceptable.
- Fast signals allow a short gate of about 30 ns.
- It has a very good spatial resolution of $\approx 40 - 60\mu$m.
- At the moment relatively large $30\times30\text{cm}^2$ detectors are being built for the experiments COMPASS and HERA-B. The latter should operate at a flux of about $0.25\times10^7/\text{cm}^2/\text{s}$.
- Complex detector shapes can be naturally arranged.
- Two projections readout is possible.
- It is thin in radiation lengths (below 0.3% per 2 coordinates).

The momentum resolution which a set of GEM detectors would provide was simulated. 5 GEM double coordinate planes (in the shape of rings) were distributed in the space of 40-120 cm from the target center. The readout stripes were nearly radial, at the 10° stereo angle. At the minimal radius of the ring, the spatial resolution assumed was 40μm in ϕ direction, while dropping linearly with the radius.

In a field of 2 T the trajectory of a particle with the transverse momentum of 1 GeV/c is bent with a curvature of 150 cm. The momentum resolution calculated is as follows:

P GeV/c	θ	$\sigma P/P$
2.	30°	1.3%
5.	20°	3.3%
9.5	10°	6.7%

The charged particle flux was simulated in the same was as the energy flow for the calorimeter described in section 3.5.3. At the lowest radius in the detector plane closest to the target a flux of $\sim 5 \times 10^6/\text{s}/\text{cm}^2$ at 1μA which is close to the limit.

The occupancy predicted is about 3%.

In total, about 3.5 m^2 of GEM detectors is needed, which would have about 20k of readout channels.

The detector described should be able operate at the beam currents up to $\sim 2\mu$A.

3.5.5 Hodoscope

The main purpose of the hodoscope is to provide the best timing possible. Another task - to suppress the events caused by high energy photons should be performed well by the tracking detectors. The trigger will be based mainly on the calorimeter signals above a certain threshold. However, the calorimeters existing or being built at JLab at the moment provide a time resolution not better than 4-5 ns due to the type of PMT used. The hodoscope should be as highly segmented as possible in order to provide an acceptable occupancy. It is preferential to use a lucite Cherenkov counter instead of a scintillator counter in order to reduce the response to low energy particles. Such a hodoscope is being built for Real

Compton experiment at Hall A. The time resolution of 1 ns can be achieved. The expected occupancy of the hodoscope shown on Figure 3 with 180 elements is ~10% within a 30 ns time window and about 1.% with the 2 ns minimal time resolution of CEBAF, at 1μA.

The detector described should be able operate at the beam currents up to $\sim 2\mu$A.

3.5.6 Acceptance and event rates

The acceptance of the detector was calculated using GEANT simulation. For the event rate evaluation it is assumed that the detector is running with a mixed untagged beam of 0.5μA at 11 GeV, with a 6% RL radiator, on a 10 cm liquid hydrogen target.

In order to minimize the errors of the evaluation, the results of the Cornell experiment [5] were used, scaled for the difference in the integrated luminosity and the acceptances. The end point of the Cornell experiment was at 11.8 GeV, while the end point at JLab would be 11.0 GeV. Assuming the J/ψ(1S) cross-section energy dependence of Formula (1), with n=2, and that the JLab experiment has the same amount of equivalent quanta on the same target as the Cornell experiment, the J/ψ(1S) production yield at JLab would be 50% of the Cornell. If n=0 in Formula (1), the yield would be 70% of the Cornell. We assume a correction factor for the JLab to Cornell ratio of 0.5.

meaning	Cornell, 1975	JLab proposal
Duty cycle	0.07	1.
End point, GeV	11.8	11.
Beam	γ	e^-
e^- beam current, radiator	-	0.5μA, 0.06
N equivalent quanta, average, s^{-1}	3.3×10^9	1.9×10^{11}
Target	2.9 g/cm^2 Be	0.7 g/cm^2 LH
Days of running	11.4	90*0.7=63
Acceptance	≈ 0.03	≈ 0.3
End point correction factor	1.	0.5
Relative J/ψ(1S) yield	1.	$\times$380
Relative mass resolution	1.	$\times$0.5
J/ψ(1S) / BG	500/100	$\sim 2\cdot10^5/2\cdot10^4$
Magnetic field	0.85kGs·m dipole	20kGs solenoid
$\mathcal{L}$, γp, in spill, cm^{-2}s^{-1}, E$_\gamma$ >5 GeV	7.0×10^{34}	6.3×10^{34}
Recoil detected?	no	yes
Full kinematics	no	yes

Table 4: Comparison of the proposed experiment at JLab and the experiment at Cornell

The beam current of 0.5μA was selected in order to equalize the J/ψ(1S)p luninosity with the "in-spill" luminosity of the Cornell experiment. In these conditions the experiment at JLab should be able to accumulate about 400 times higher statistics than at Cornell. The gains come from the duty cycle of CEBAF, from the detector acceptance and the duration of running.

The direct esimate of the $J/\psi(1S)$ yield, done in in the same way as described for the "standard spectrometers" (see section 2), gave $\sim 1 \cdot 10^5$ particles for a 90 day run - about 50% of the yield obtained by scaling from the Cornell experiment.

The influence of the electron component of the beam should be considered. The simulation shows that the low energy particles from the electron beam do not create an unacceptable load on the detectors up to the beam current of $\sim 2\mu$A. However, the high energy particles may affect the trigger or add a considerable background to the mass spectra. Two types of processes were evaluated for 0.5μA:

- The e^- beam produces additionally about $2.5 \cdot 10^4$/s scattered e^- at E>1.5GeV in $10^\circ < \theta < 30^\circ$. The accidental coincidence rate should be still under control.
- The pion rate from the e^- beam should be about 2 times higher than in Cornell experiment, where it made no visible contribution to the background.

The advantages with respect to the Cornell experiment are summarized:

– higher statistics (about $\times 400$);

– the better energy and mass resolution ($\times 3$) and also the full kinematic information on the event should reduce the background;

– the full kinematic information should exclude the inelastic processes, which could contribute about 30% to the Cornell sample;

– the γ energy can be reconstructed with a resolution of about 1% - at least 2 times better than at Cornell.

We used a coservative limit of 0.5μA for the beam current. It is likely that the experiment would be able to use up to 2μA.

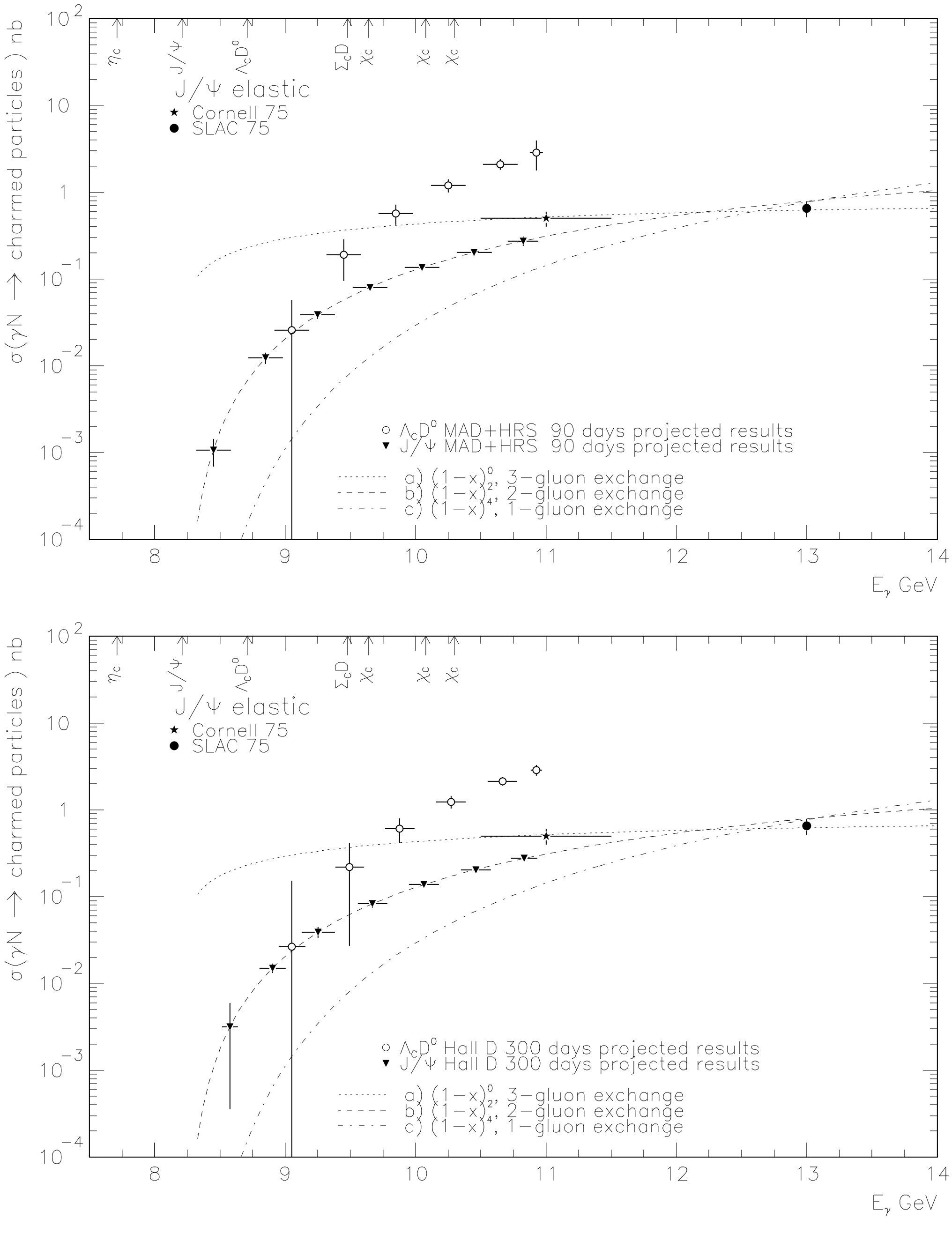

Figure 2: Expected results for the cross-section measurements with MAD+HRS on the top plot and Hall D on the bottom plot, assuming the cross-section behavior described by (1). The theoretical curves were normalized to the existing measurements at 11 and 13 GeV. On the top of the plots the thresholds of various charm channels are shown.

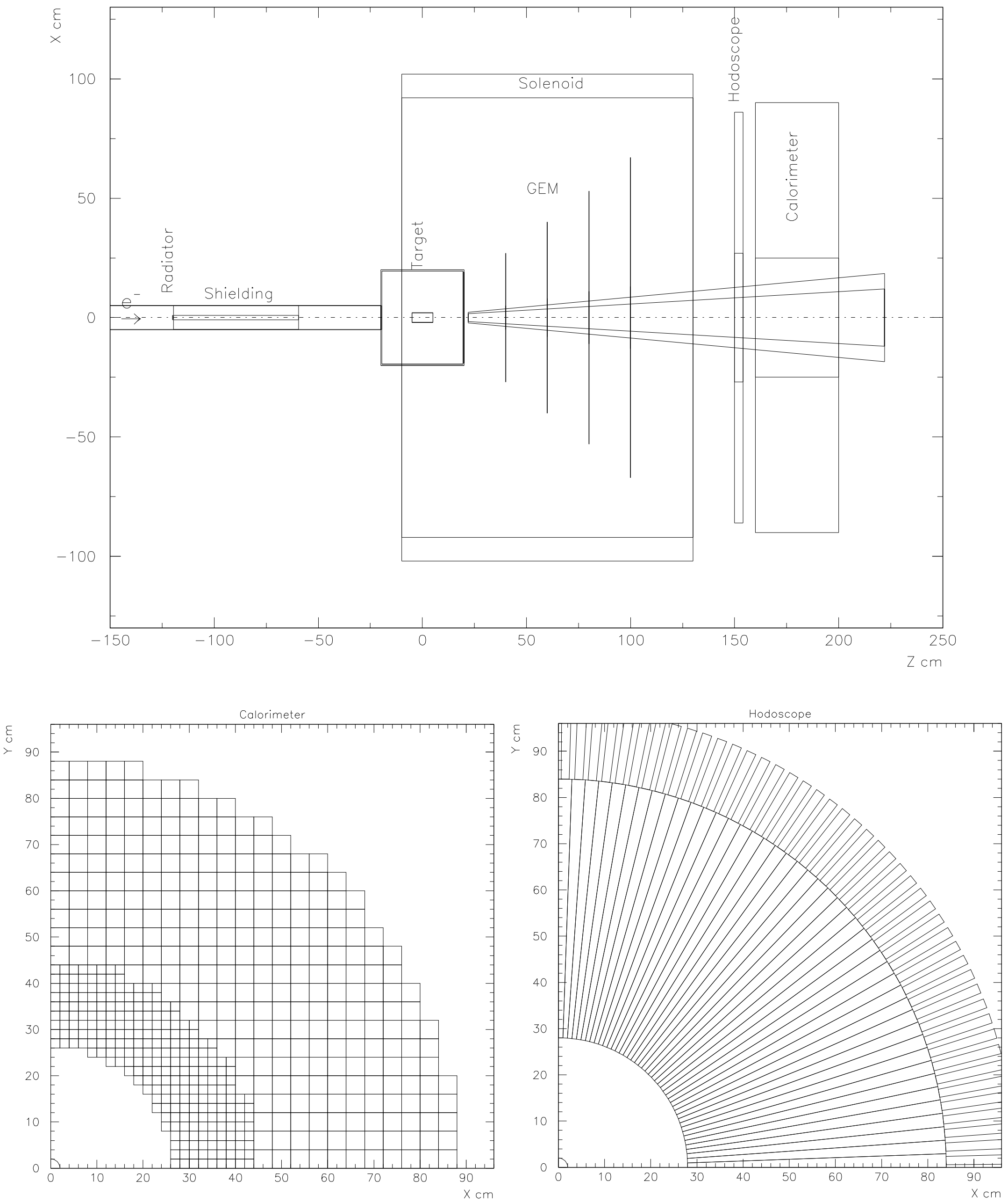

Figure 3: Layout of the dedicated detector proposed for the J/ψ(1S) studies. On the top picture a general layout is shown, while on the two bottom pictures a frontal look on one quadrant of the calorimeter and one quadrant of the hodoscope is presents.

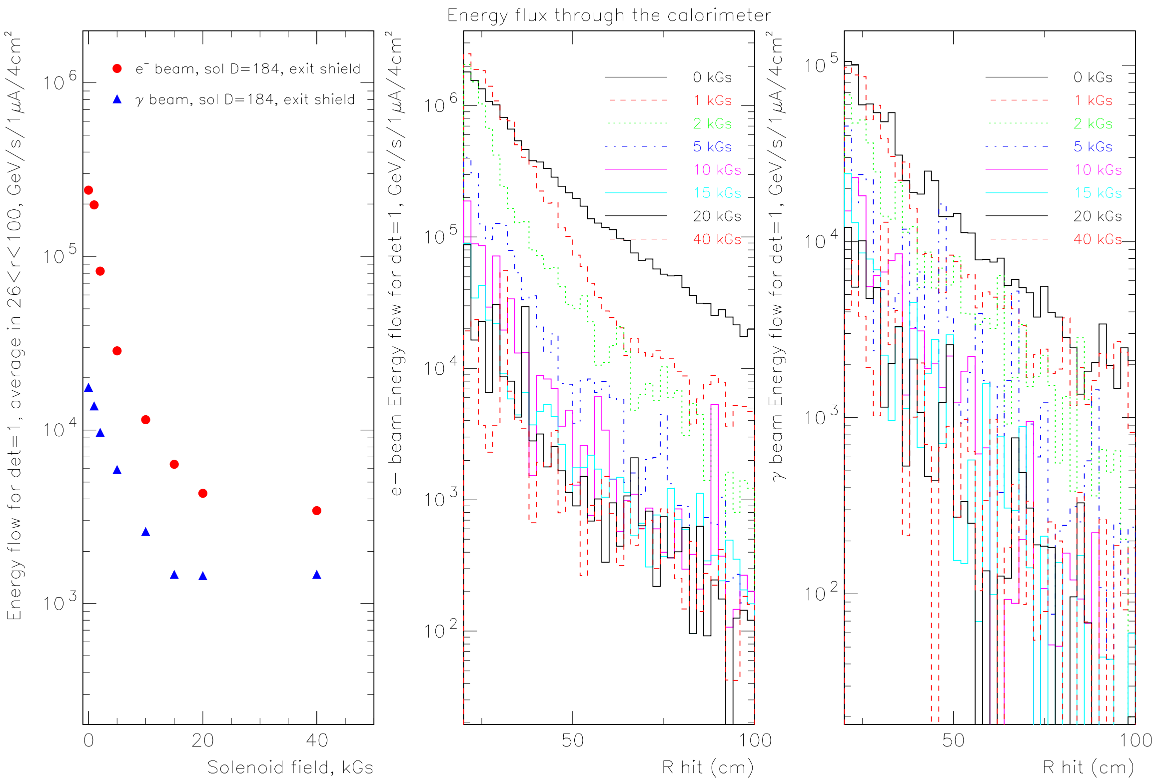

Figure 4: The GEANT simulation of the energy flow on the calorimeter face through a 4×4 cm^2 area for 1μA electron beam. The flux was calculated in two cases - for a mixed beam of electrons and photons and for a pure photon On the left plot the average fluxes over the calorimeter surface is presented, depending on the field in the solenoid. On the middle plot the flux dependence on the distance from the beam for various values of the field is shown for the mixed beam, while the right plot shows the same values for the pure photon beam.

References

[1] S. J. Brodsky, P. Hoyer, C. Peterson and N. Sakai, Phys. Lett. **B93**, 451 (1980).

[2] S. Frixione, M. L. Mangano, P. Nason and G. Ridolfi, Nucl. Phys. **B412**, 225 (1994) [hep-ph/9306337].

[3] D. Kharzeev, H. Satz, A. Syamtomov and G. Zinovjev, Eur. Phys. J. **C9**, 459 (1999) [hep-ph/9901375].

[4] U. Camerini *et al.*, Phys. Rev. Lett. **35**, 483 (1975).

[5] B. Gittelman, K. M. Hanson, D. Larson, E. Loh, A. Silverman and G. Theodosiou, Phys. Rev. Lett. **35**, 1616 (1975).

[6] B. Knapp *et al.*, Phys. Rev. Lett. **34**, 1040 (1975).

[7] R. L. Anderson *et al.*, Phys. Rev. Lett. **38**, 263 (1977).

[8] R. L. Anderson, SLAC-PUB-1741 *Invited talk presented at Int. Conf. on Production of Particles with New Quantum Numbers, Wisconsin U., Madison, Apr 22-24, 1976.*

[9] D. Aston *et al.*, Phys. Lett. **B94**, 113 (1980).

[10] M. Binkley *et al.*, Phys. Rev. Lett. **48**, 73 (1982).

[11] K. Abe *et al.*, Phys. Rev. Lett. **51**, 156 (1983).

[12] K. Abe *et al.* [SLAC Hybrid Facility Photon Collaboration], Phys. Rev. **D30**, 1 (1984).

[13] B. H. Denby *et al.*, Phys. Rev. Lett. **52**, 795 (1984).

[14] M. D. Sokoloff *et al.* [Fermilab Tagged Photon Spectrometer Collaboration], Phys. Rev. Lett. **57**, 3003 (1986).

[15] R. Barate *et al.* [NA14 Collaboration], Z. Phys. **C33**, 505 (1987).

[16] M. I. Adamovich *et al.* [Photon Emulsion Collaboration], Phys. Lett. **B187**, 437 (1987).

[17] J. C. Anjos *et al.* [Tagged Photon Spectrometer Collaboration], Phys. Rev. Lett. **65** (1990) 2503.

[18] M. P. Alvarez *et al.* [NA14/2 Collaboration], Z. Phys. **C60**, 53 (1993).

[19] P. L. Frabetti *et al.* [E687 Collaboration], Phys. Lett. **B316**, 197 (1993).

[20] C. Adloff *et al.* [H1 Collaboration], hep-ex/0003020.

[21] G. Theodosiou, B. Gittelman, K. M. Hanson, D. Larson, E. Loh and A. Silverman, Phys. Rev. Lett. **37**, 126 (1976).

[22] Y. Lemoigne *et al.*, Phys. Lett. **B113**, 509 (1982).

[23] R. Clark *et al.* [Hall D Collaboration], Design Report, 1999.

[24] F. Sauli, Nucl. Instrum. Meth. **A386** (1997) 531.

[25] S. Bachmann, A. Bressan, L. Ropelewski, F. Sauli and D. Mormann, Nucl. Instrum. Meth. **A433**, 464 (1999).

[26] S. Bachmann, A. Bressan, A. Placci, L. Ropelewski and F. Sauli, CERN-EP-99-148 *Prepared for 5th International Conference on Position Sensitive Detectors (PSD 5), London, England, 13-17 Sep 1999.*

[27] GEANT 3.21 CERN Program Library W5103, CERN 1998